

Dynamics of red blood cells in microporous membranes

Justyna Czerwinska,^{1,a)} Michael Rieger,¹ and Dominik E. Uehlinger²

¹Artorg Center for Biomedical Engineering, University of Bern, Murtenstrasse 50, CH-3010 Bern, Switzerland

²Department of Nephrology, Hypertension and Clinical Pharmacology, University of Bern, Inselspital, Bern, Switzerland

(Received 23 April 2014; accepted 19 June 2014; published online 2 July 2014)

We have performed microfluidic experiments with erythrocytes passing through a network of microchannels of 20–25 μm width and 5 μm of height. Red blood cells (RBCs) were flowing in countercurrent directions through microchannels connected by μm pores. Thereby, we have observed interesting flow dynamics. All pores were blocked by erythrocytes. Some erythrocytes have passed through pores, depending on the channel size and cell elasticity. Many RBCs split into two or more smaller parts. Two types of splits were observed. In one type, the lipid bilayer and spectrin network were cut at the same time. In the second type, the lipid bilayer reconnected, but the part of spectrin network stayed outside the cell forming a rope like structure, which could eventually break. The microporous membrane results in multiple breakups of the cells, which can have various clinical implications, e.g., glomerulus hematuria and anemia of patients undergoing dialysis. The cell breakup procedure is similar to the one observed in the droplet breakage of viscoelastic liquids in confinement. © 2014 AIP Publishing LLC. [<http://dx.doi.org/10.1063/1.4886967>]

I. INTRODUCTION

Lipid bilayer membrane conformations were extensively studied during past decades.¹ Erythrocyte vesiculation² and entire cells' merging^{3,4} were also investigated through years. Additionally, the tether extrusion from red blood cells (RBC) with the length up to 25 μm was performed.^{5–7} The vesiculation of RBCs during blood storage is often observed.⁸ Locally, the erythrocyte membrane deforms due to pH changes.⁹ Several methods were implemented to measure erythrocyte membrane properties: AFM,¹⁰ SEM,¹¹ high frequency electric field,¹² optical tweezers,¹³ and micropipette experiments with actin filaments visualizations.¹⁴ Moreover, models for elastic behavior of spectrin network were developed.¹⁵ It depends significantly on the shape as well as on general health of an erythrocyte (parasite infection).¹⁶ It was shown that echinocytes transition has not altered cell membrane stiffness significantly.¹⁷ The theory of the vesicle shape transition was developed many decades ago, and relies on the optimal surface curvature and on the cell volume to surface ratio.¹⁸ The static shape of erythrocyte is a result of the minimum of the membrane's bending energy.¹⁹ Dynamic shapes and their transition are much more complicated and up to now not entirely understood. Some experiments studied the transport of microcapsule through small micropores such as droplet flow through membrane with 1 μm pores,²⁰ part of RBC was sucked up into the 0.4 μm pore,²¹ and RBCs were flown through a 2.7 $\mu\text{m} \times 3 \mu\text{m}$ channel on a microchip.²² In clinical practice, it was observed that RBCs can pass the glomerular membrane²³ and that the glomerular bleeding results in RBC deformed shapes in the urine.²⁴ Glomerular membrane has pores of the size below 1 μm .²⁵ The large shear rate deformations of RBC ghosts (cells from which the hemoglobin is removed) were studied also by theory.²⁶ The breakup of the erythrocytes observed in our experiments

^{a)} Author to whom correspondence should be addressed. Electronic mail: justyna.czerwinska@artorg.unibe.ch.

was similar to the one of viscoelastic jets. The breakup of the fluidic jets were studied widely,²⁷ e.g., in the confinement of the microchannel²⁸ and in the various viscoelastic regimes.²⁹

II. EXPERIMENTAL SETUP

The experiment we have performed is unique, as the setup design forces erythrocytes to be in one alignment (5 μm channel high) and the structure of the flow and membrane leads to large RBC deformations. This results in very interesting flow dynamics.

We have performed experiments in a microfluidic chip using 7 days old blood samples from a blood bank. This is one of the youngest samples possible to obtain, after blood processing. The cells should be of the similar properties to the one of the fresh blood. However, some echinocytes were present in the sample. The flow of cells in the microchip was investigated under the microscope (see Figures 1(b) and 1(c)). Movies were recorded with a camera with a frequency of 25 fps. The magnification used varied, but for result presentation we show pictures with 400 \times and 1000 \times magnification. The microchip was connected to a syringe pump by tube of 1.2 mm diameter. The flow rate was 0.1 $\mu\text{l/h}$. The actual flow depends strongly on the hematocrit level, which cannot be easily controlled. Fahraeus-Lindqvist effect leads to changes in the viscosity of blood. Hence, even with uniform pumping, the flow of RBCs is non-uniform in hematocrit level and velocity of a single cell. Studies were performed over few days and for each case a new sample (7 days old) from the blood bank was obtained. The blood sample from the blood bank was prepared in SAGM solution.³⁰ The RBC concentrate was then dissolved in normal saline solution to obtain a hematocrit of 10%, which is a common value for capillary flow. To avoid blood coagulation sodium citrate from S-Monovette was added.

The microchips were designed using Comsol Multiphysics software and then translated to AutoCAD (see Figure 1(d)). The file was sent to Stanford University Foundry, and there the mask and microchip were manufactured in polydimethylsiloxane (PDMS), with no additional surface utilization. The PDMS chip was sealed with glass with oxygen plasma technique. The obtained channel height was 5 μm and the width varied between 20 and 25 μm . Two large channels were connected with the set small microchannels forming an environment, which is referred as a porous membrane (see Figure 1(d)). Pore length was between 2 μm and 14 μm . Pore width, when it was possible to measure, was around 0.5 μm and above. The pore size estimation was obtained from video analysis using Matlab. The pores have rather rectangular structure due to the chip manufacturing. The pore distribution was not a uniform one in location and sizes. We have tested four different microchips. The scheme of the flow is shown in Fig. 1(c). The RBCs flow in opposite directions in the two microchannels (countercurrent flow), and the microchannels are connected by μm -pores. In the situation when the flow was in the same direction no crossing of a pore was observed. An example of the basic flow characteristics can be seen in Fig. 1(e) (Multimedia view). Depending on pore size and pore distribution various flow patterns are observed. Generally, cells tend to fill an empty pore instantaneously. Very often several cells are observed at one location. Blood samples are composed of a large amount of echinocytes. However, if the shear rate is large, the shapes of the cells are not distinguishable (see Fig. 2(e)). The blood sample is relatively young in comparison to the maximal blood storage time of 41 days, hence, there is no evidence that the mechano-elastic properties of our sample vary significantly from the one of the fresh blood sample.

III. RESULTS AND DISCUSSION

Fig. 2 shows a series of time frames for various events. The majority of cells are traveling through the microchannel loop. However, when the pressure difference is high and when one of the pores opens, it is immediately blocked by another RBC. Fig. 2(a) shows RBC passing through the pore. Depending on the size of the cell and initial cell localization, the travel through pore can happen in less than one second to several seconds. The cell is unaltered after passing through the pore (Multimedia view). Fig. 2(b) shows the RBC passing through a pore, but at this occurrence it splits into two parts. The parts are not equal in size and also differ in shape (Multimedia view). Fig. 2(c) shows the channel where already one cell is present and

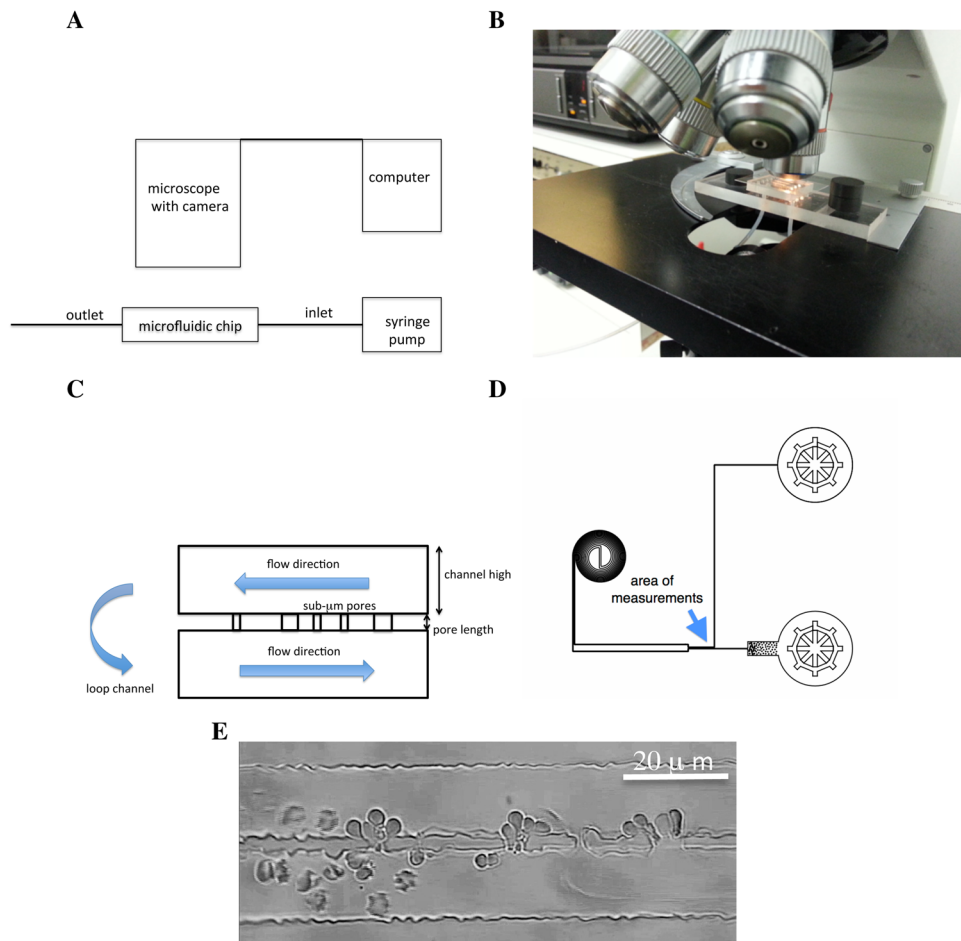


FIG. 1. (a) Experimental setup overview. (b) Microfluidic chip under the microscope. (c) The scheme of the measurement area. The flow directions are indicated by arrows. The μm pores have non-uniform distribution in a location, density, and sizes. In the loop, channel flow is directed from the top to the bottom. (d) AutoCAD microchip design. (e) The example of the flow of the erythrocytes in $400\times$ magnification. The movies corresponding to these pictures are S1 and S2. (Multimedia view) S1: [URL: <http://dx.doi.org/10.1063/1.4886967.1>], S2: [URL: <http://dx.doi.org/10.1063/1.4886967.2>]

second one enters. Then the split of RBC occurs. Fig. 2(d) shows a cell entering the channel and then the split occurs. However, in this case, the cell reconnects. Finally, Fig. 2(e) presents the transformation of the echinocyte to the slippery shape RBC due to the increase in the shear rate. Similar shapes for erythrocytes in high shear were often observed.³¹ It helps to understand that despite the fact that blood used in experiments was consisting of many echinocytes, the cells in most of the figures look like fresh blood. It was observed that even after split when the cell moves into the low velocity region it recovers the echinocyte characteristics.

Fig. 3 again shows a split of RBCs but a different type than the one presented in Fig. 2. In both cases, the lipid bilayer breaks, but in this case, the remaining spectrin network only breaks partially. Hence, it forms a rope, which connects two parts of the cell. Fig. 3(a) shows a split of a single erythrocyte. Fig. 3(b) shows a situation similar to Fig. 2(c), but the cell remains connected by a rope. Similarly, Fig. 3(c) shows a split with a remaining spectrin rope but at larger magnification and higher flow velocity. Hence, the shape after the split looks like a slippery RBC. Fig. 3(d) shows double a split. The difference lies in a fact that parts of the cell are connected by rope. In that case, the cell has split into three parts. One part is left on the other side of the membrane, and the remaining two parts are connected by rope. The spectrin rope is quite a stable structure, but can be broken by a very fast flow. The spectrin network connects spectrin fibers in rest position (70 nm long). The elasticity of that structure is large, as each one can stretch up to 200 nm without breaking up.¹⁵ Hence, the observed rope is very elastic. Fig. 3(e)

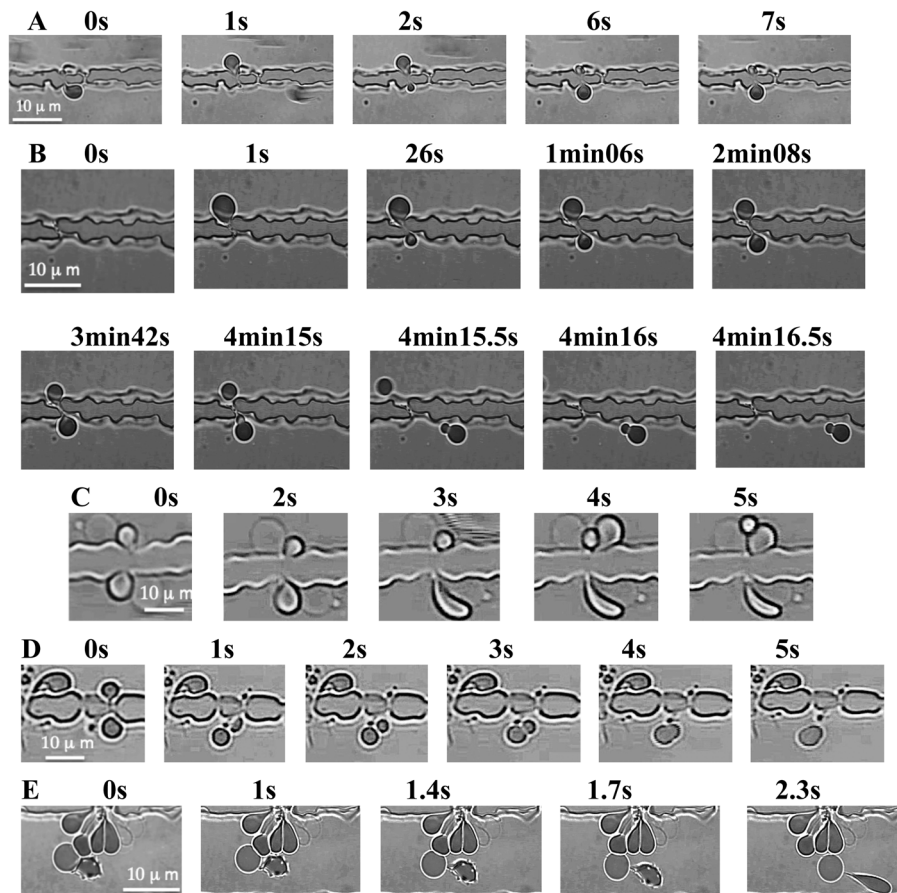


FIG. 2. Figure shows the flow of RBCs in a microchannel in the vicinity of the microporous membrane. The flow on top of the membrane is from right to left and on the bottom of the membrane from left to right. Most of the RBCs pass along and only a few go through the pores. (a) Time sequence of the erythrocyte passing through a pore. (b) The time sequence of an erythrocyte passing through a pore and splitting into two separate cells. (c) The time sequence of an erythrocyte passing through a pore and splitting, when the channel is already occupied by another erythrocyte. (d) The time sequence of an erythrocyte passing through a pore, splitting into two separate cells, and reconnecting again to one cell. (e) The time sequence of an erythrocyte and an echinocyte. The echinocyte undergoes high shear stress and changes into a slippery shape. The echinocyte is connected to the second cell and drags it along. (Multimedia view) [URL: <http://dx.doi.org/10.1063/1.4886967.3>] [URL: <http://dx.doi.org/10.1063/1.4886967.4>]

shows that the spectrin rope can be visible, very long and that the remaining parts of the cell make satellites, which with time travel along the rope and reach the main cell again (Multimedia view). A similar behavior was observed by tether extrusion.⁵⁻⁷

The passage of the RBCs through the microporous membrane leads to cell transformations. Many of them pass without changes, some result in ghost cells, and some break into two or more parts. The cell breakage resulting in cell ghosts were not that often observed. The remains of the membrane can be easily washed out (easier than the full cell). Hence, these are more difficult to spot after transition. However, the breakage in the vast majority of cells does not lead to ghosts. The lipid bilayer reconnects fast enough to avoid hemoglobin leakage. Statistics on ghost cell formation was not performed. Most of the cells were either passing intact or when split the membrane reconnected immediately. The statistics of cell transitions can be seen on Fig. 4(a). There are several types of split or passing events. The most simple is the passing of an intact cell (see Fig. 2(a)) or a split to two cells (Fig. 3(b)). However, in most of the cases, pore is already occupied by several other cells. Hence, the split events occur in the presence of other cells or when a rope from the spectrin network is formed. Examples of all types of cell transition are also shown in this figure. The split of cells most likely occurs when other cells are also in the pore. The cell fit is then tighter, but also the interaction of the cells membranes

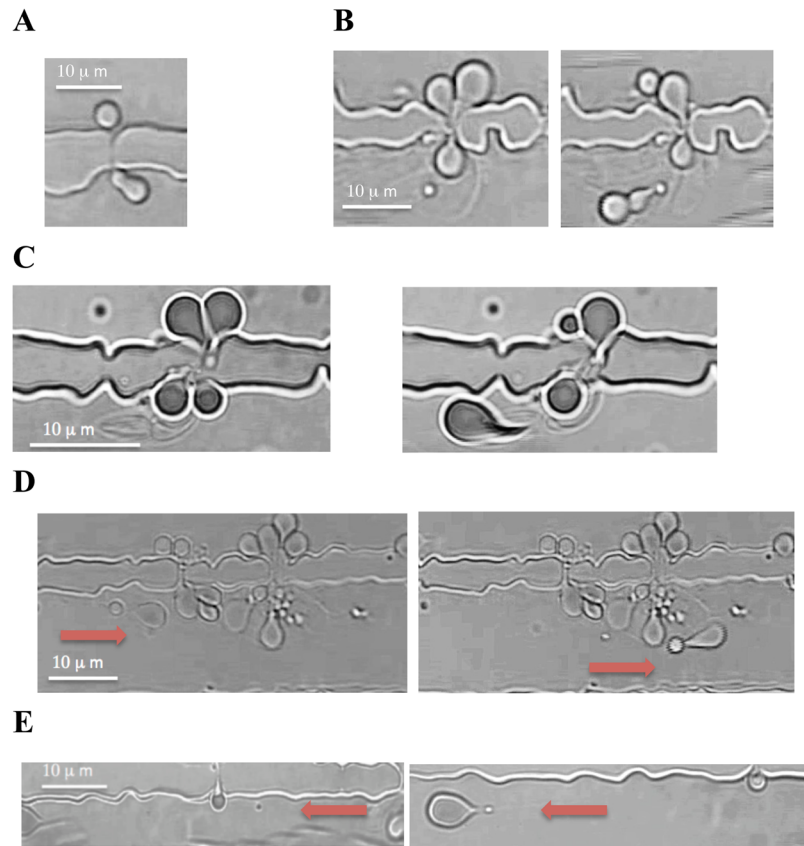


FIG. 3. RBC dynamics related to the cytoskeleton breakup. A spectrin network separates and forms a rope like structure, which connects the remaining parts. With the increase of flow velocity, the rope breaks. (a) Single RBC breakup with a remaining rope. (b) Two RBCs in a pore. One is breaking up with a remaining rope (two time frames). (c) Two RBCs breakup with a remaining rope (two time frames) with the higher shear flow. (d) Multiple RBCs breakup (two time frames). One has a particularly long rope and satellite structures (see arrow). (e) Two time frames of a single RBC breakup with a remaining rope and satellite RBC parts, which in time are joining the main cell. (Multimedia view) [URL: <http://dx.doi.org/10.1063/1.4886967.5>] [URL: <http://dx.doi.org/10.1063/1.4886967.6>] [URL: <http://dx.doi.org/10.1063/1.4886967.7>]

between each other leads to the increase of viscoelastic effects leading to a breakup. Fig. 4(b) shows the membrane characteristics for all the cases presented in Fig. 4(a).

The types of the pass/breakup events are also presented in Fig. 5 as a function of time and pore length L and pore width w . The clean pass and split events (without other cells in the channel and without rope formation) are distinguishably divided into two regions. A longer time spent by a cell in a pore of the same pore characteristics leads to the split (Fig. 5(a)). Additionally, it can be seen that the majority of events do not lead to cell breakage. This is not the case when several cells are in the channel (Fig. 5(b)) and the spectrin network does not break (a rope is formed). In such a case, most of the cells break. The time scale is much shorter than the one for clean split though. For the case when other cells are present in the channel and no rope is formed, the number of pass events and splits are about the same. The time the cell spends in a pore will however be larger for events resulting in a split. This statistics does not take into account the fact that erythrocytes will have slightly different sizes and membrane characteristics. This might result in differences between event types for the same pore.

The difficulty in characterization of the erythrocyte breakup lies in the fact that each cell has slightly different properties. A blood sample generally consists of cells of various ages (up to 120 days). The older cells are denser, smaller, and the membrane is slightly stiffer. Hence, each cell has different properties, which cannot be easily estimated during our experiments. Other experiments, however, indicate some average values for RBC. Example can be found in Table I.

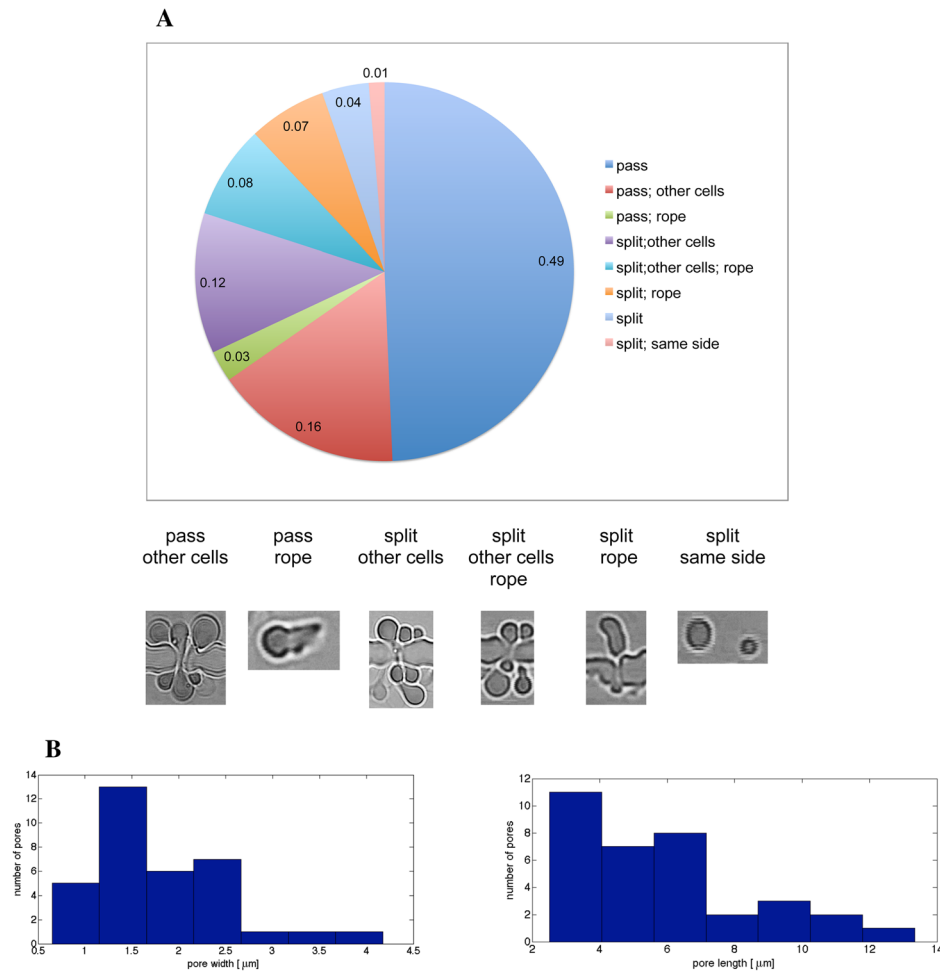


FIG. 4. (a) The diagram represents the percentage of events observed in the membrane. It can be noted that due to the various sizes of the membrane pores cells pass unchanged most of the time also if other cells are already occupying a pore. The pictures represent the terminology of the event. The pass and split are shown in Fig. 2. The split events represent 32% of all events and are more common when other cells are already occupying the pore. (b) Histograms of membrane characteristic (pore width and length distribution) for all events presented in (a). It must be noted that cell split or pass was sometimes measured on the same pore several times.

The split of the cell can be seen at the level of a whole cell and at the level of the structure of the RBC membrane. The cell membrane consists of a lipid bilayer and a spectrin network. The latter one occupies 10% of the surface.¹⁰ The spectrin chains have a length of about 200 nm,³² but they are folded in the RBC resulting in a length from 35 to 100 nm.¹⁰ Hence, during the stretching each chain can expand about three times. The bonding between the sites of spectrin complexes (dimers, tetramers, hexamers, etc.) can easily be broken and reconnected.¹¹ The same is true for a lipid bilayer. It can break and reconnect easily. The lysis tension for the lipid bilayer is about 10 mN/m,³³ at a pH similar to the physiological environment. Similarly, for RBC, the lysis tension is about 10–12 mN/m, and also depends on the spectrin network binding³⁴ and on the solution in which the cells are immersed. Hence, at the level of the RBC membrane split and connect events can occur easily and sometimes are spontaneous, e.g., vesiculation during blood storage.⁸

At the level of the whole cell, erythrocyte behavior in a pore is similar to the one observed for liquid droplets passing through microchannels. To estimate the physical regimes, which are guiding the process, several flow properties were estimated (see Table II). It can be seen that the Reynolds number is very small, as expected. The time scales responsible for a breakup such as Rayleigh and viscous time differ by several orders of magnitudes, and also from the cell

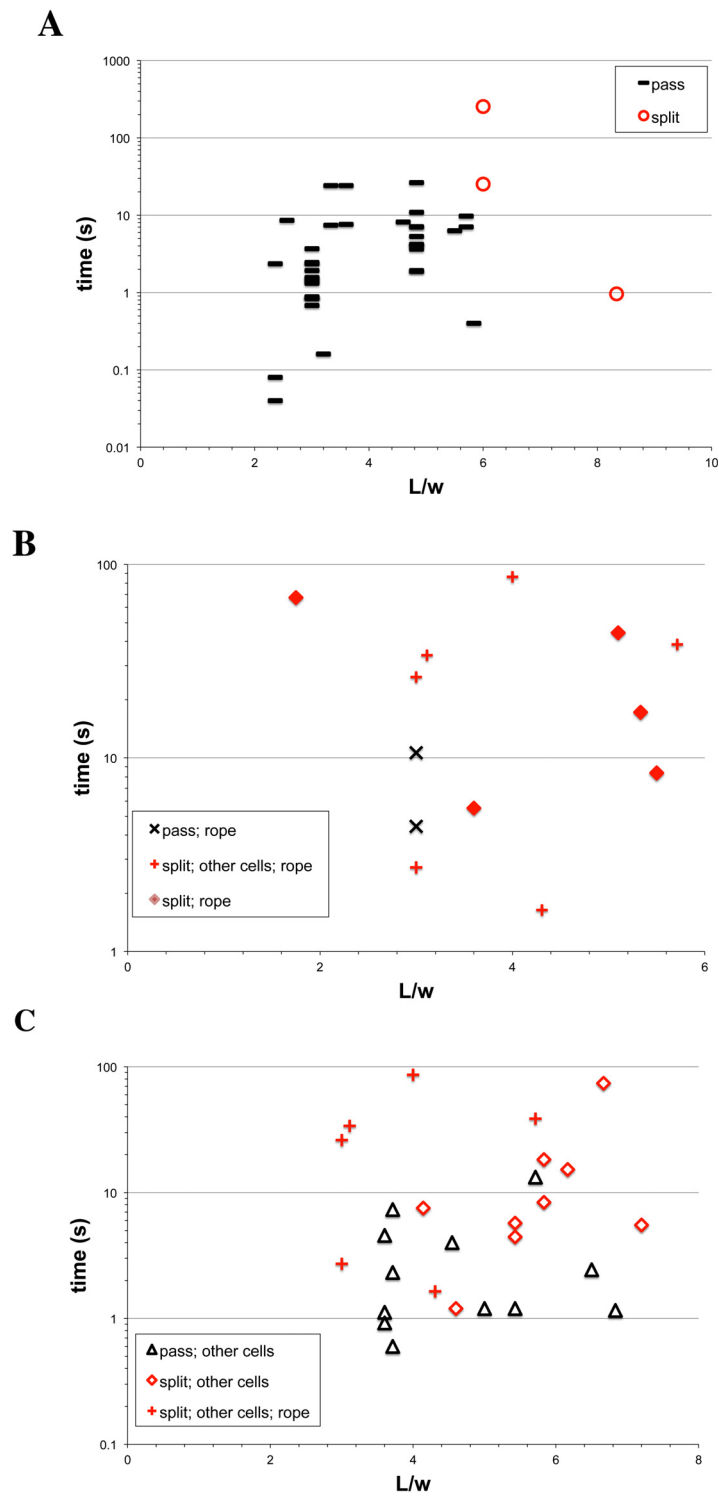


FIG. 5. Plots indicating events in relation to the length L and width w of the pore and the cell's transit time. (a) Only clean events are shown. It can be seen that the majority of cells are passing through the pore. (b) The events, when the cells are influenced by the pore, and form an attaching rope from the spectrin network. Most of these events lead to cell breakage. (c) Events, when the pore is already occupied by cells, and other cells are entering the same pore. In such a case some cells pass untouched and some break. These, which are faster, are more likely to pass unchanged.

TABLE I Erythrocyte characteristic parameters.

Property		Type of cell	Value	References
Erythrocyte density	ρ		1063–1130 kg/m ³	35
Cytoplasmic viscosity (20 °C)	η	No hemoglobin	2 – 3 mPa·s	36
(37 °C)		27% hemoglobin	50 mPa·s	37
Membrane viscosity (24 °C)			0.34 μ N·s/m	12
			6.1 μ N/m	12
Membrane shear modulus (24 °C)	μ		2.5 μ N/m	38
		Young	5 μ N/m	39
		Old	12 μ N/m	39
			280 ms	38
Relaxation time	τ	Young	120 ms	39
		Old	640 ms	39

relaxation time. It can be seen that the flow in the pore is heavily influenced by the viscoelastic properties of the cell. Hence, the breakup will be similar to the one of viscoelastic fluids. It can indeed be observed that cells sometimes have satellite hemoglobin droplets similar to the jet breakage presented in Ref. 29 (see Figs. 3(b), 3(d), and 3(e)).

To quantitatively analyze the breakup, we have looked at the model theory presented in Ref. 28. The breakup criterion was derived from the studies of microdroplets in T-junction in a lab on a chip device. The critical capillary number Ca combining viscosity, surface tension, and characteristic flow velocity was related to the geometrical dimensions

$$Ca = L/w \left(\frac{1}{(L/w)^{2/3}} - 1 \right)^2. \quad (1)$$

Assuming in our case that $Ca = \eta V / \sigma$, where $V = A/t$ and length A is a result of the cell squeezing through the pore (2D case because all cells were align the same in our experiments due to the channel dimensions): $A \cdot w = \pi R^2$. R is a cell radius chosen as $4 \mu\text{m}$. Taking $w = 0.5 \mu\text{m}$ leads to $A = 0.1 \text{ mm}$. The values from Table I and rewriting the above equation leads to coefficient $\alpha = 0.08 - 2$ and Eq. (1) can be written as below:

$$t = \frac{\alpha}{L/w \left(\frac{1}{(L/w)^{2/3}} - 1 \right)^2}. \quad (2)$$

The line plotted in Fig. 6 is given by Eq. (2) and coefficient $\alpha = 2$.

TABLE II. Characteristic problem dimensions. Definitions given from the literature.²⁹

Property	Equation	Value range
Capillary velocity	$V_{cap} = \mu / \eta$	0.05–6 mm/s
Radius of the channel	R_0	0.5–1 μm
Rayleigh time	$t_R = \sqrt{\rho R_0^3 / \mu}$	3.3–21.3 μs
Viscous break-up time	$t_v = 14.1 \eta R_0 / \mu$	1.18–282 ms
Inertia time scale	$t_i = 1.95 t_R$	6.5–41.2 μs
Weissenberg number	$Wi = \tau V_{cap} / R_0$	6–768
Reynolds number	$Re = \rho \mu R_0 / \eta^2$	$0.5 - 339 \times 10^{-6}$
Deborah number	$De = \tau / t_R$	$0.06 - 1.9 \times 10^5$

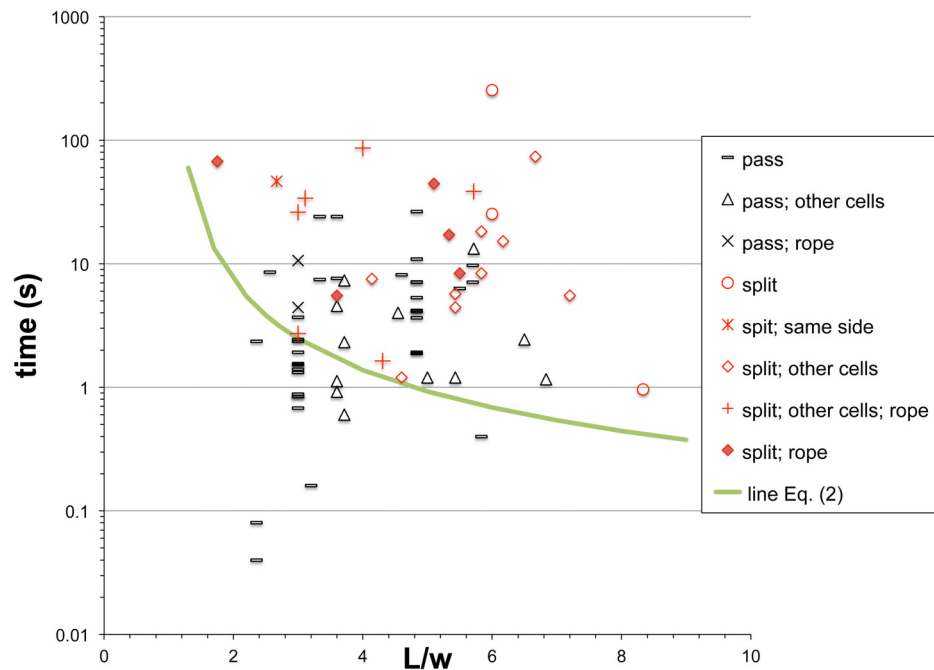


FIG. 6. All types of events as a function of the ratio of the length L and width w of the pore in the time of the event. It can be seen that faster cells are more likely to pass unchanged. There is a region where cells are equally likely to pass or split and the top right part of the graph leads to the split. The theoretical line predicting splitting region (Eq. (2)) is also shown. It relates to the liquid droplets breakup theory.²⁸

Figure 6 shows all events (pass and split) as a function of pore characteristics (length L and width w) and the cell passing time. It can be seen that the breakup of the cells is indeed similar to the one observed in droplets.²⁸ The L/w ratio and the time determine the regions specific for the breakage or passing of the erythrocyte. The fit is quite good taking into account that cells have different dimensions and elasto-mechanical properties. In case of droplets, the parameters can be easier controlled. The region, which determines if the cell passes or breaks, is more spread than the one for droplets. Hence, the plotted fit line is just the reference to underline the main trend characteristics.

The last figure (Fig. 7) shows some cells shapes after breakup. Two issues need to be noticed. The shape recovery will depend on the cell membrane properties but also on the process how the split has occurred. Fig. 7(a) shows a cell, which has a long recovery time, and is attached by a rope formed from a spectrin network. In addition, cells do not split to two equals most of the time, but that depends on the particular flow parameters. Example cases are shown in Fig. 4(a). Many small cells have spherical shape Fig. 7(b). Spherocytes are stiffer than discocytes.¹⁶ Despite the fact that they are small, they do not pass pores of the same size due to their

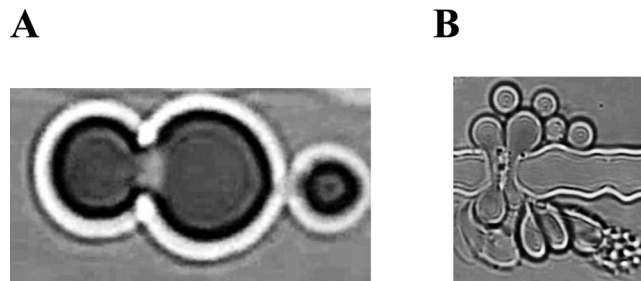


FIG. 7. Example of cells after passing through pores. (a) The cell did not break but has changed shape, and the shape is quite slow to recover. (b) Multiple small round cells are the remains after the breakup of other cells.

stiffness. These observations lead to the conclusion that the cells, in general, will not only change their size but also their visco-elastic properties. However, this remains to be investigated by some other experimental methods.

IV. CONCLUSION

We have presented the behavior of RBCs in the vicinity of microporous membranes. It leads to various interesting effects such as cell split or rope formation. The cells break similarly to viscoelastic droplets. The flow is highly influenced by viscosity and the membrane shear modulus. In general, the majority of cells pass the membrane intact, even though the cells in a relax form are of much larger membrane diameter. However, some erythrocyte split and this event significantly depends on the speed of the observed process. If the cell stays longer in the pore, then it tends to break. The channels are non-uniform. The initial cell position also varies as well as cell size and elasto-mechanical properties. Therefore, the same channel can lead to various types of passing/breakup configurations. After breakup, the cells have different dimensions and visco-elastic properties (relaxation recovery time). Taking into account, the fact that in many extracorporeal devices as well as in the human body RBCs are moving in the vicinity of microporous membranes, the same dynamics should be observed. Examples that such situations can occur are glomerular hematuria or RBCs passing through dialyzer membranes. The cells remain affected and this may lead to anemia, because erythrocytes become stiffer and smaller.

The allocation of the cells can have also a role in the breakup characteristics. In our experiments, the cells were all elongated into one position due to the microchip design restriction (5 μm channel height). However, in general, erythrocytes can pass through microporous membrane in various positions. It has been observed that this can happen in glomeruli.²³ In such a case, the cells are aligned with different conformation. There are two principal conformations related to the axes of the symmetry. In the case of 3D allocation, the other conformation (perpendicular to the one investigated by us) will be observed. Both conformation will have a different curvature minimization diagram¹⁸ and therefore will lead to different split. The second conformation and the passage through a membrane such as the glomerulus can lead to a split and cell deformation as observed (disc with small satellites)²⁴ and used to diagnose glomerular hematuria.

We have shown that the flow of the erythrocytes in the presence of the microporous membrane is very complicated and leads to various types of events. The importance of the RBC behavior has large clinical implications and membranes of such type are often encountered by the cells. This topic has not been extensively investigated by other researchers. Therefore, our work is trying to address this issue in more precise manner.

¹M. Lipowsky, "The conformation of membranes," *Nature* **349**, 475 (1991).

²D. W. Knowles, L. Tilley, N. Mohandas, and J. A. Chasis, "Erythrocyte membrane vesiculation: Model for the molecular mechanism of protein sorting," *Proc. Natl. Acad. Sci. U.S.A.* **94**, 12969–12974 (1997).

³Y. Wu, J. D. Rosenberg, and A. E. Sowers, "Surface shape change during fusion of erythrocyte membranes is sensitive to membrane skeleton agents," *Biophys. J.* **67**, 1896–1905 (1994).

⁴M. Baumann, "Dynamics of oscillating erythrocyte doublets after electrofusion," *Biophys. J.* **77**, 2602–2611 (1999).

⁵R. M. Hochmuth, N. Mohandas, and P. L. Blackshear, Jr., "Measurement of the elastic modulus for red cell membrane using a fluid mechanical technique," *Biophys. J.* **13**(8), 747–762 (1973).

⁶R. M. Hochmuth, H. Wiles, E. Evans, and J. McCown, "Extensional flow of erythrocyte membrane from cell body to elastic tether. II. Experiment," *Biophys. J.* **39**(1), 83–89 (1982).

⁷N. Borghi and F. Brochard-Wyart, "Tether extrusion from red blood cells: Integral proteins unbinding from cytoskeleton," *Biophys. J.* **93**, 1369–1379 (2007).

⁸A. G. Kriebardis, M. Antonelou, K. E. Stamoulis, E. Economou-Peterse, L. H. Margaritis, and I. S. Papassideri, "RBC-derived vesicles during storage: Ultrastructure, protein composition, oxidation, and signalling components, transfusion," *Transfus.* **48**, 1943–1953 (2008).

⁹M. Bobrowska-Hagerstrand, H. Hagerstrand, and A. Iglic, "Membrane skeleton and red blood cell vesiculation at low pH," *Biochem. Biophys. Acta* **1371**, 123–128 (1998).

¹⁰M. Takeuchi, H. Miyamoto, Y. Sako, H. Komizu, and A. Kusumi, "Structure of the erythrocyte membrane skeleton as observed by atomic force microscope," *Biophys. J.* **74**(5), 2171–2183 (1998).

¹¹S.-C. Liu, L. H. Derick, and J. Palek, "Visualization of the hexagonal lattice in the erythrocyte membrane skeleton," *J. Cell Biol.* **104**, 527–536 (1987).

¹²H. Engelhardt and E. Sackmann, "On the measurement of shear elastic moduli and viscosities of erythrocyte plasma membranes by transient deformation in high frequency electric fields," *Biophys. J.* **54**(3), 495–508 (1988).

- ¹³J. Sleep, D. Wilson, R. Simmons, and W. Gratzer, "Elasticity of the red cell membrane and its relation to hemolytic disorders: An optical tweezers study," *Biophys. J.* **77**(6), 3085–3095 (1999).
- ¹⁴J. C.-M. Lee, D. T. Wong, and D. E. Discher, "Direct measurement of large, anisotropic strains in deformation of the erythrocyte cytoskeleton," *Biophys. J.* **77**, 853–864 (1999).
- ¹⁵J. C. Hansen, R. Skalak, S. Chien, and A. Hoger, "Spectrin properties and the elasticity of the red blood cell membrane skeleton," *Biorheology* **34**(4/5), 327–348 (1997).
- ¹⁶M. Dao, C. T. Lim, and S. Suresh, "Mechanics of the human red blood cell deformed by optical tweezers," *J. Mech. Phys. Solids* **51**, 2259–2280 (2003).
- ¹⁷K. Zeman, H. Engelhard, and E. Sackmann, "Bending undulations and elasticity of the erythrocyte membrane: Effects of cell shape and membrane organization," *Eur. Biophys. J.* **18**(4), 203–219 (1990).
- ¹⁸U. Seifert, "Configurations of fluid membranes and vesicles," *Adv. Phys.* **46**(1), 13–137 (1997).
- ¹⁹P. B. Canham, "The minimum energy of bending as a possible explanation of the biconcave shape of the human red blood cell," *J. Theor. Biol.* **26**, 61–81 (1970).
- ²⁰E. van der Zwan, K. Schron, K. van Dijke, and R. Boom, "Visualization of droplet break-up in pre-mix membrane emulsification using microfluidic devices," *Colloids Surf., A* **277**, 223–229 (2006).
- ²¹E. Ogura, P. J. Abatti, and T. Moriizumi, "Measurement of human red blood cell deformability using a single micropore on a thin Si₃N₄ film," *IEEE Trans. Biomed. Eng.* **38**(8), 721–726 (1991).
- ²²D. J. Quinn, I. Pivkin, S. Y. Wong, K.-H. Chiam, M. Dao, G. E. Karniadakis, and S. Suresh, "Combined simulations and experimental study of large deformation of red blood cells in microfluidic system," *Ann. Biomed. Eng.* **39**(3), 1041–1050 (2011).
- ²³J. E. Collar, S. Ladva, T. D. H. Cairns, and V. Cattell, "Red cell traverse through thin glomerular basement membranes," *Kidney Int.* **59**, 2069–2072 (2001).
- ²⁴H. Kohler, E. Wandel, and B. Brunck, "Acanthocyturia - A characteristic marker for glomerular bleeding," *Kidney Int.* **40**, 115–120 (1991).
- ²⁵F. Jørgensen, *The Ultrastructure of the Normal Human Glomerulus* (Munksgaard, Copenhagen, 1966).
- ²⁶C. D. Eggleton and A. S. Popel, "Large deformation of red blood cell ghosts in a simple shear flow," *Phys. Fluids* **10**(8), 1834–1845 (1998).
- ²⁷J. Eggers and E. Villermaux, "Physics of liquid jets," *Rep. Prog. Phys.* **71**, 036601 (2008).
- ²⁸D. R. Link, S. L. Anna, D. A. Weiz, and H. A. Stone, "Geometrically mediated breakup of drops in microfluidic devices," *Phys. Rev. Lett.* **92**(5), 054503 (2004).
- ²⁹L. E. Rodd, T. P. Scott, J. J. Cooper-White, and G. H. McKinley, "Capillary break-up rheometry of low-viscosity elastic fluids," *Appl. Rheol.* **15**, 12–27 (2005).
- ³⁰J. R. Hess, "An update on solutions for red cell storage," *Vox Sang.* **91**(1), 13–19 (2006).
- ³¹H. L. Goldsmith and J. Marlow, "Flow behavior of erythrocytes. I. rotation and deformation in dilute suspensions," *Proc. R. Soc. B* **182**, 351–384 (1972).
- ³²D. M. Shotton, B. E. Burke, and D. Branton, "The molecular structure of human erythrocyte spectrin: Biophysical and electron microscopic studies," *J. Mol. Biol.* **131**(2), 303–329 (1979).
- ³³H. V. Ly, D. E. Block, and M. L. Longo, "Interfacial tension effect of ethanol on lipid bilayer rigidity, stability, and area/-molecule: A micropipet aspiration approach," *Langmuir* **18**, 8988–8995 (2002).
- ³⁴E. A. Evans, R. Waugh, and L. Melnik, "Elastic area compressibility modulus of red cell membrane," *Biophys. J.* **16**(6), 585–595 (1976).
- ³⁵S. L. Schrier, E. Rachmilewitz, and N. Mohandas, "Cellular and membrane properties of alpha and beta thalassemic erythrocytes are different: Implication for differences in clinical manifestations," *Blood* **74**(6), 2194–2202 (1989).
- ³⁶P. D. Morse, D. M. Luszczakowski, and D. A. Simpson, "Internal microviscosity of red blood cells and hemoglobin-free resealed ghosts: A spin-label study," *Biochem.* **18**(22), 5021–5029 (1979).
- ³⁷A. C. Allison, "Properties of sickle-cell haemoglobin," *Biochem. J.* **65**, 212–219 (1957).
- ³⁸K. Bambardekar, J. A. Dharmadhikari, D. Mathur, S. Sharma, and A. K. Dharmadhikari, "Measuring erythrocyte deformability with fluorescence, fluid forces, and optical trapping," *J. Biomed. Opt.* **13**(6), 064021 (2008).
- ³⁹S. K. Mohanty, A. Uppal, and P. K. Gupta, "Optofluidic stretching of RBCs using single optical tweezers," *J. Biophoton.* **1**, 522–525 (2008).